Heliyon 10 (2024) e24236

Contents lists available at ScienceDirect

Heliyon

journal homepage: www.cell.com/heliyon

Research article

Identifying the prognosis implication, immunotherapy response prediction value, and potential targeted compound inhibitors of integrin subunit α3 (ITGA3) in human cancers

Jiawei Gui [a,e,1], Lufei Yang [a,b,c,d,1], Junzhe Liu [a,b,c,d,1], Yishuang Li [f], Mi Zou [g], Chengpeng Sun [e], Le Huang [e], Xingen Zhu [a,b,c,d], Kai Huang [a,b,c,d,*]

[a] Department of Neurosurgery, The 2nd Affiliated Hospital, Jiangxi Medical College, Nanchang University, Nanchang, Jiangxi 330006, PR China
[b] Institute of Neuroscience, Jiangxi Medical College, Nanchang University, Nanchang, Jiangxi 330006, PR China
[c] Jiangxi Key Laboratory of Neurological Tumors and Cerebrovascular Diseases, Nanchang, PR China
[d] JXHC Key Laboratory of Neurological Medicine, Jiangxi, 330006, Nanchang, PR China
[e] HuanKui Academy, Jiangxi Medical College, Nanchang University, Nanchang 330031, PR China
[f] Queen Mary School, Jiangxi Medical College, Nanchang University, Nanchang, PR China
[g] The Second Clinical Medical College, Jiangxi Medical College, Nanchang University, Nanchang 330031, PR China

ARTICLE INFO

Keywords:
Integrin subunit α3 (ITGA3)
Pan-cancer
Biomarker
Tumor microenvironment
Immunotherapy
Molecular docking

ABSTRACT

The integrin subunit α3 (ITGA3) is a member of the integrin alpha chain protein family, which could promote progression, metastasis, and invasion in some cancers. Still, its function in the tumor microenvironment (TME), cancer prognosis, and immunotherapy remains unclear. A multifaceted analysis of ITGA3 in pan-cancer utilizing various databases and online web tools revealed ITGA3 was aberrantly expressed in tumor tissues and upregulated in most cancers, which may be related to ITGA3 genomic alterations and methylation modification. In addition, ITGA3 was significantly correlated with the poor or better prognosis of cancer patients, immune-related pathways in hallmark, immune infiltration, and immune checkpoints, revealing a biological function of ITGA3 in the tumor progression, tumor microenvironment, and tumor immunity. We also found that ITGA3 could predict the response to tumor immunotherapy based on cytokine-treated samples and immunotherapy cohorts. ITGA3 may participate in shaping and regulating the tumor microenvironment to affect the tumor immune response, which was a promising immunotherapy response predictive biomarker and potential therapeutic target to work synergistically with cancer immunotherapy to boost the response and efficacy. Finally, potential targeted compound inhibitors and sensitive drugs were screened using databases ConnectivityMap (CMap) and CellMiner, and AutoDock Tools was used for molecular docking.

1. Introduction

Despite the great advances in cancer treatment over the past decades, especially immunotherapy, which has tremendously

* Corresponding author. Department of Neurosurgery, The 2nd Affiliated Hospital, Jiangxi Medical College, Nanchang University, Nanchang, Jiangxi 330006, PR China.
E-mail address: kaihuang@ncu.edu.cn (K. Huang).
[1] These authors contributed equally to this work.

https://doi.org/10.1016/j.heliyon.2024.e24236
Received 29 May 2023; Received in revised form 30 November 2023; Accepted 4 January 2024
Available online 6 January 2024

revolutionized cancer treatment, patients with advanced malignant tumors still suffer from unsatisfactory prognoses [1]. Therefore, exploring new prognostic biomarkers and therapeutic targets for cancer is urgent. Increasingly, researchers are realizing the complex tumor microenvironment (TME), especially the tumor immune microenvironment (TIME), is the main factor for the poor prognosis of cancer patients [2,3]. The deadly tumor microenvironment creates a powerful advantage for the development of cancer.

Integrins are cell surface adhesion receptors that mediate the interactions between extracellular matrix (ECM) and cells, playing a crucial role in cell migration and maintenance of tissue homeostasis [4]. The integrin family consists of 18 α subunits and 8 β subunits, which could combine in various combinations to form 24 distinct integrins [5]. Recently, dysregulated integrin signaling, which is overly activated in the tumor microenvironment, and could positively impact tumor immunobiology, has gradually been taken seriously [4,6]. Integrins have emerged as promising targets for the development of cancer treatment [7,8]. As a member of the integrin alpha chain protein family, ITGA3 forms a heterodimer with a β1 subunit to constitute an integrin capable of interacting with extracellular matrix proteins [5]. Several previous studies have analyzed the association of ITGA3 with certain cancers. Research shows that ITGA3 may be closely related to drug resistance, metastasis, proliferation, and poor prognosis of ovarian cancer [9]. ITGA3 was upregulated in both colorectal cancer cell lines and tissues, and the upregulation of ITGA3 counteracted the tumor suppressive effect of elevated levels of miR-199a-5p [10]. Furthermore, ITGA3 was associated with the proliferative, invasive, migratory, and autophagic phenotypes of esophageal squamous cell carcinoma cells [11], as well as the stemness and invasiveness of glioblastoma cells [12]. To date, the expression levels and roles of ITGA3 in most human cancers remain elusive, and a comprehensive analysis regarding the functional and clinical implications of ITGA3 at a pan-cancer level is still lacking. Additionally, the potential mechanisms of ITGA3 in the tumor immune microenvironment and tumor immunotherapy have not been fully explored.

This study systematically investigated the prognosis implication and immunotherapy response prediction value of ITGA3 at the pan-cancer level. The purpose of our investigation is to comprehensively analyze the expression levels, functions, and clinical implications of ITGA3 in multiple human cancers, as well as explore its potential role in the tumor immune microenvironment and tumor immunotherapy. We aim to provide a new biomarker and target for cancer treatment and to provide a novel member for integrin-targeted immunotherapy.

2. Materials and methods

2.1. Dataset acquisition and processing

The cancer cell lines' transcriptomic data were obtained from the Cancer Cell Line Encyclopedia (CCLE) platform (https://sites.broadinstitute.org/ccle/). The log2 (TPM+1) transformed and normalized mRNA expression profile and related clinical data were downloaded from the Cancer Genome Atlas (TCGA) and Genotype Tissue-Expression (GTEx) databases via UCSC Xena (http://xena.ucsc.edu/). The immunotherapy cohorts of urothelial cancer patients (IMvigor210) and melanoma patients (GSE91061 and GSE78220) were separately collected from https://www.nature.com/articles/nature25501 and Gene Expression Omnibus (GEO) (https://www.ncbi.nlm.nih.gov/geo/). Perturbagens (compound molecules) that give rise to opposing expression signatures to ITGA3 were downloaded from the CMap database (https://clue.io/).

2.2. Protein localization, interaction, and expression validation of ITGA3

The Clinical Proteomic Tumor Analysis Consortium (CPTAC) data obtained from UALCAN [13] (http://ualcan.path.uab.edu/) was utilized to explore ITGA3 expression at the protein level in human cancers. The "subcellular" section of the Human Protein Atlas (HPA, https://www.proteinatlas.org/) database was used to display the ITGA3 protein's subcellular distribution images of immunofluorescence in two different cell lines (U-251 and A-431). The ITGA3 protein interaction network analysis was implemented through the Compartmentalized Protein-Protein Interaction (ComPPI, https://comppi.linkgroup.hu/) database. Representative immunohistochemistry (IHC) staining of ITGA3 (Antibody: HPA008572) in tumors and corresponding normal tissues was obtained from the HPA database.

2.3. Genomic alteration and methylation analyses of ITGA3

In this study, ITGA3 gene's alteration frequencies of diverse genomic alteration types were analyzed via cBioPortal (http://www.cbioportal.org/). The tumor mutation burden (TMB) and microsatellite instability (MSI) in human cancers were calculated using the R package "maftools". Spearman's method was used to analyze the correlation of ITGA3 expression with TMB and MSI. Moreover, the correlation between ITGA3 mRNA expression and methylation or copy number variation (CNV) in pan-cancer was analyzed by the Gene Set Cancer Analysis (GSCA, http://bioinfo.life.hust.edu.cn/GSCA/) web tool. The methylated CpG islands most associated with ITGA3 expression in each cancer type were identified from GSCA, and their prognostic values in the respective cancers were analyzed by MethSurv [14].

2.4. Prognostic analysis

Data obtained from the UCSC Xena database, which included information on ITGA3 mRNA expression and clinical prognosis of patients with various cancer types, was utilized to evaluate the prognosis implication of ITGA3 using the following outcome measures: Overall survival (OS), disease-specific survival (DSS), disease-free interval (DFI), and progression-free interval (PFI). We conducted

univariate Cox regression and Kaplan-Meier analysis to investigate the prognostic predictive function of ITGA3 and determined the cutoff of the Kaplan-Meier curve analysis using the function "surv-cutpoint" from "survminer" R package (0.4.9).

2.5. Definition of low- and high-ITGA3 subgroups to ascertain differentially expressed genes (DEGs)

To ascertain DEGs across diverse cancer types between subgroups with varying levels of ITGA3 expression, we classified patients into high- and low-ITGA3 subgroups based on their respective ITGA3 mRNA expression levels. Specifically, patients in the top 30 % were designated as high-ITGA3 subgroup, while those in the bottom 30 % were classified as low-ITGA3 subgroup. The "limma" R package was utilized to compute the fold change (log2-base) and the adjusted p-value of DEGs. DEGs for 33 types of cancer are presented in Table S1.

2.6. Gene Set Enrichment Analysis (GSEA)

Gene Set Enrichment Analysis (GSEA) is a computational method that determines whether an a priori defined set of genes shows statistically significant, concordant differences between two biological states (In this study, we analyzed the low- and high-ITGA3 subgroups) [15]. Calculation of the Normalized Enrichment Score (NES) and False Discovery Rate (FDR) in 33 cancer types was based on the hallmark gene set file (h.all.v7.4.symbols.gmt) obtained from Molecular Signatures Database (MSigDB, https://www.gsea-msigdb.org/gsea/index.jsp). The R package "clusterProfiler" [16] was used to implement the GSEA, and the R package "ggplot2" was utilized to summarize the outcomes in a bubble plot.

2.7. Immune infiltration analysis of ITGA3 in pan-cancer

the "Gene" module of the database Tumor Immune Estimation Resource 2.0 (TIMER 2.0, http://timer.cistrome.org/) was used to explore the association of ITGA3 with the immune infiltration level in TCGA pan-cancer project. 21 immune cell subsets were involved including eosinophil (Eos), B cells, cancer-associated fibroblasts (CAFs), common lymphoid progenitors, myeloid progenitors, granulocyte-monocyte progenitors, myeloid-derived suppressor cell (MDSCs), dendritic cells, endothelial cells (Endo), hematopoietic stem cells (HSCs), $CD4^+$ T cells, neutrophils, γδT, NK cells, natural killer T cell (NKT), T cell follicular helper (Tfh), macrophages, monocytes, $CD8^+$ T cells, mast cells, and regulatory T cells (Tregs). Visualized outcomes were displayed on a heatmap via the R package "ggplot2". The website Comprehensive Analysis on Multi-Omics of Immunotherapy in Pan-cancer (CAMOIP) provides a platform for screening various prognostic markers and analyzing the mechanisms underlying their association with tumor immunotherapy [17]. Based on CAMOIP website, we compared two groups (high- and low-ITGA3 expression groups) of immune-related scores (Intratumor Heterogeneity, Lymphocyte Infiltration Signature Score, Macrophage Regulation, TGF-β Response, and Stromal Fraction).

2.8. Single-cell analysis of ITGA3

The database CancerSEA (http://biocc.hrbmu.edu.cn/CancerSEA/home.jsp) aims to provide a functional state atlas of cancers at single-cell level to comprehensively decode functional states in diverse cancer types [18]. The relevance between ITGA3 expression level and 14 functional states in diverse cancer types was obtained using cancerSEA. Moreover, Tumor Immune Single-cell Hub 2 (TISCH2, http://tisch.comp-genomics.org/home/) web tool was employed to reveal ITGA3 expression levels quantificationally in immune cells, stromal cells, and malignant cells.

2.9. Immune checkpoints and immune subtypes correlation investigation of ITGA3

In this study, we analyzed the correlation of immune checkpoints derived from a previous study [19] with ITGA3 expression in pan-cancer. Moreover, the association between ITGA3 expression and immune subtypes was analyzed by the "Subtype" module of TISDB, a tumor-immune system interaction online web portal [20] (http://cis.hku.hk/TISIDB/). ITGA3 expression levels of these subtypes in different cancers are presented visually.

2.10. Immunotherapy response prediction analysis

Tumour Immune Syngeneic MOuse (TISMO, http://tismo.cistrome.org/) is a database containing an extensive collection of syngeneic mouse model data specifically designed for storage, visualization, and analysis [21]. ITGA3 expression level in vivo between pre- and post-ICB treated samples, and ITGA3 expression level in vitro between pre- and post-cytokine intervened samples across cell-lines, were compared using the "Gene" module of TISMO, Wald test in DESeq2 statistically evaluated differences between groups. Comparison of the predictive power of response outcome of ITGA3 with other existing biomarkers was applied using the "Biomarker Evaluation " module of Tumor Immune Dysfunction and Exclusion (TIDE, http://tide.dfci.harvard.edu/). Additionally, we included three immune checkpoint blockade (ICB) therapy cohorts to further clarify ITGA3's response-predictive value in tumor immunotherapy. The three immunotherapy cohorts included GSE91061 (25 melanoma patients during immunotherapy with Nivolumab), GSE78220 (27 patients undergoing anti-PD1 therapy in metastatic melanoma), and IMvigor210 (298 metastatic urothelial cancer patients receiving anti-PD-L1 agent atezolizumab).

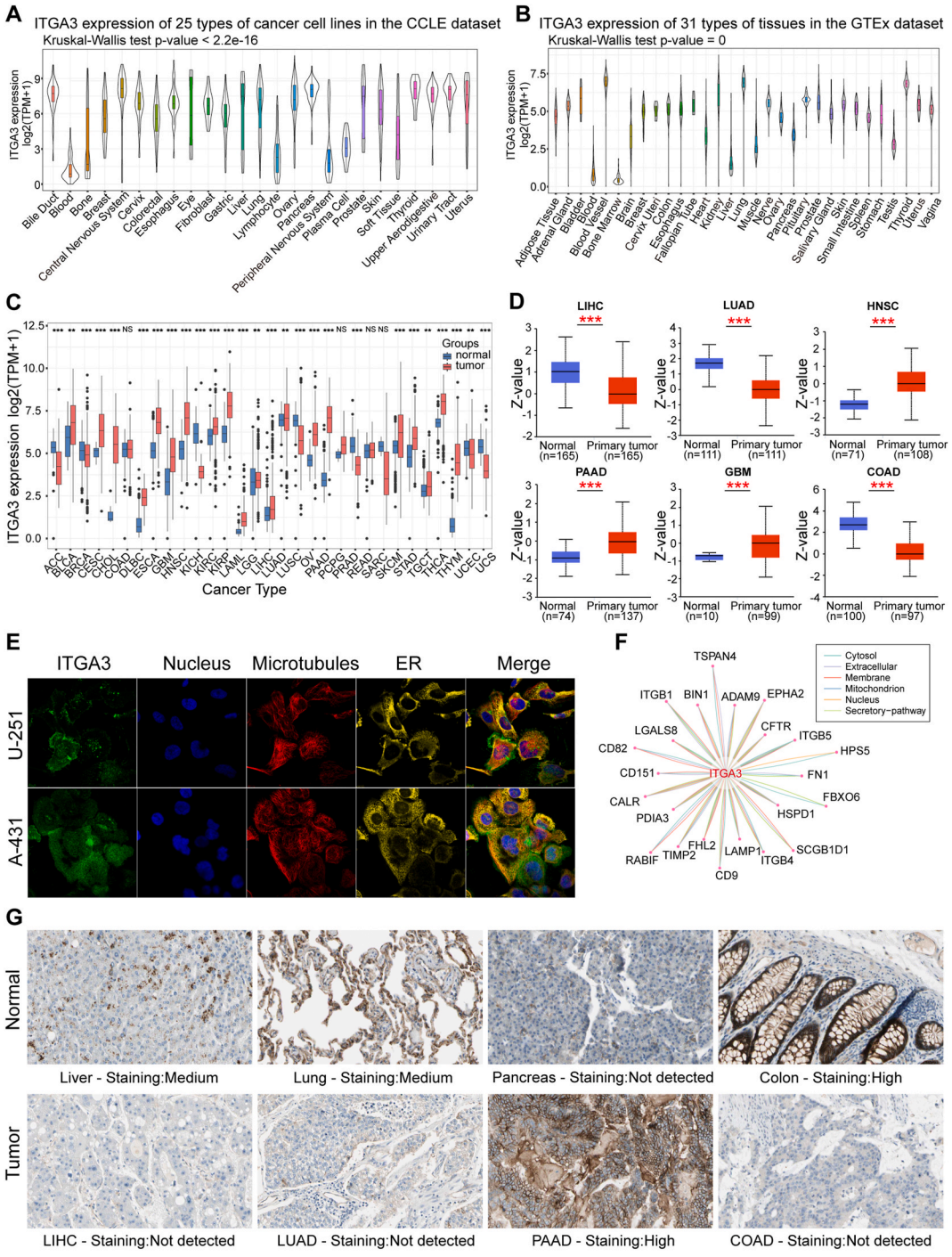

Fig. 1. Comprehensive landscape of ITGA3 expression in human cancers. (A) ITAG3 mRNA expression of 25 types of cancer cell lines in the CCLE dataset in the form of violin diagrams combined with box charts. (B) ITAG3 mRNA expression of 31 types of tissues in the GTEx dataset in the form of violin diagrams combined with box charts. (C) Box plots of the differential expression of ITGA3 mRNA between tumors and corresponding normal tissues (combining data from GTEx and TCGA databases). (D) Box plots of the protein expression (Z-value) differences of ITGA3 between normal and primary tumor tissues in 6 cancer types based on UALCAN. (E) The immunofluorescence images of ITGA3 protein, nucleus, endoplasmic reticulum (ER), microtubules, and the merged images in U-251 and A-431 cell lines. (F) The protein-protein interaction (PPI) displays an interacting network between the proteins with ITGA3. The length of the line corresponds to the interaction score, and the color of the line corresponds to the interaction distribution (membrane, extracellular, membrane, mitochondria, nucleus, and secretory pathways). (G) Immunohistochemistry (IHC) staining validation of ITGA3 protein expression levels in tumors and corresponding normal tissues based HPA database. *p < 0.05; **p < 0.01; ***p < 0.001; ns, not significant.

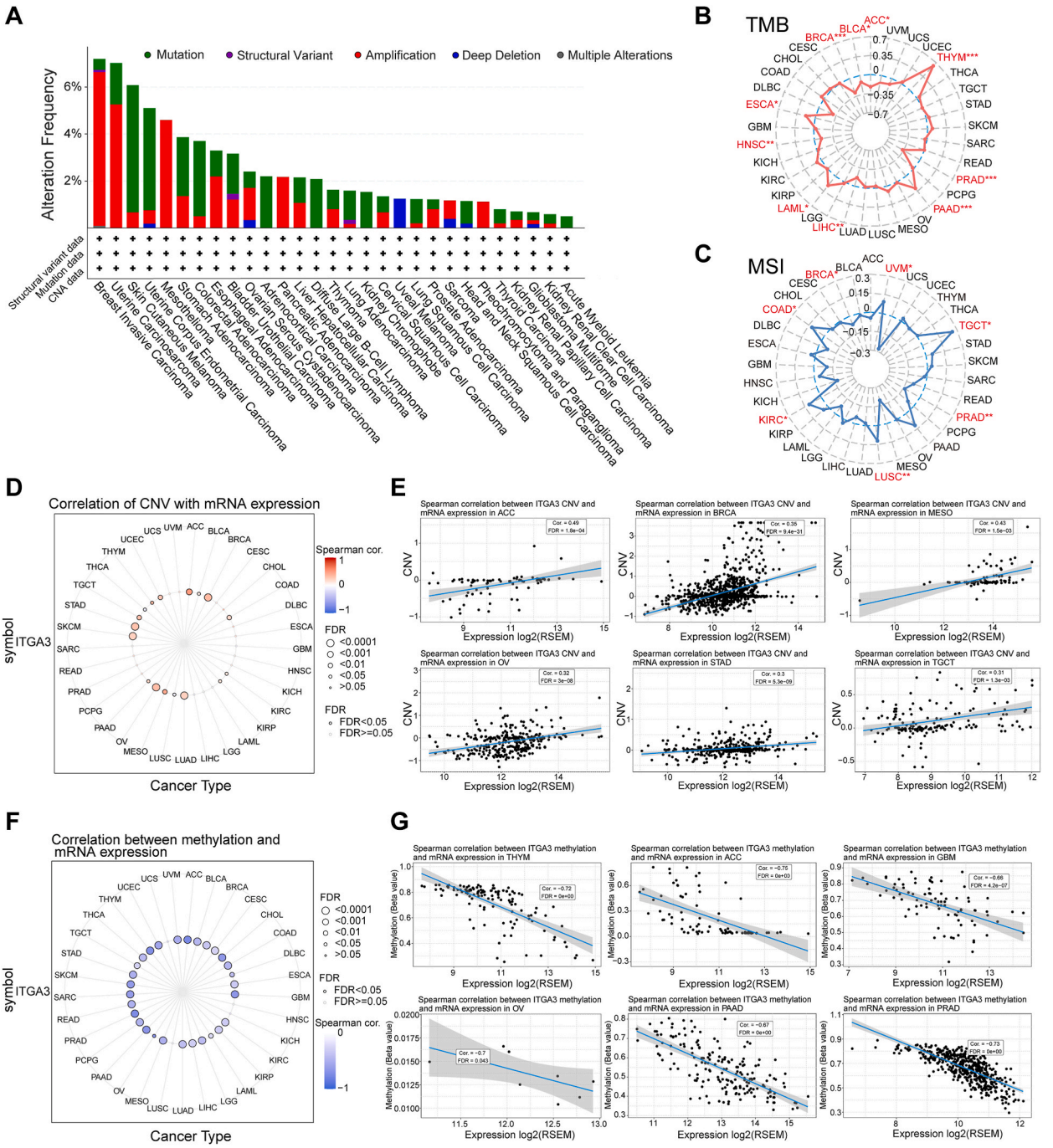

Fig. 2. ITGA3 gene is correlated with cancerous genomic alteration and methylation in pan-cancer. (A) Genomic alteration frequency of ITGA3 gene in pan-cancer according to cBioPortal database. Bar diagram classified sample data based upon genomic alteration types: mutation (green), structural variant (purple), deep deletion (blue), amplification (red) or multiple alterations (grey). "+" represents that data are available. (B) Radar chart of the correlation between ITGA3 expression and TMB. (C) Radar chart of the correlation between ITGA3 expression and MSI. (D) Bubble plot of the correlation of CNV with ITGA3 mRNA expression. (E) Scatter plots of the top six cancer types with the highest correlation scores between ITGA3 CNV and mRNA. (F) Bubble plot of the correlation of methylation with ITGA3 mRNA expression. (G) Scatter plots of the top six cancer types with the highest correlation scores between ITGA3 methylation and mRNA. (*p < 0.05, **p < 0.01, ***p < 0.001).

2.11. Potential targeted compound inhibitors screening and drug sensitivity analysis

The Connectivity Map, a drug discovery database, utilizes pattern-matching algorithms to infer functional associations between drugs, genes, and diseases based on gene expression change information [22]. We sorted DEGs between low- and high-ITGA3 subgroups according to log2 fold change to confirm up- and down-regulated genes to explore compounds that give rise to opposing expression signatures to ITGA3 based on the CMap database. Compound inhibitors were screened according to CMap score (score < -50), and negative values indicated the potential of the compounds targeting ITGA3. Potential specific compound inhibitors of ITGA3 enriched in more than 8 types of cancer and their mechanisms of action were presented. Detailed lists of compounds are presented in Table S2. Based on these potential specific inhibitors, we performed molecular docking using AutoDock Tools 1.5.7. The 3D structure of ITGA3 protein (UniProt: H2QDE3) was obtained from the AlphaFold Protein Structure Database (AlphaFold DB, https://alphafold.ebi.ac.uk/), and the 3D structures of compounds were downloaded from PubChem database (https://pubchem.ncbi.nlm.nih.gov/). The query tool CellMiner (https://discover.nci.nih.gov/cellminer/), which contains genomic and pharmacological information, was included for exploring the association of ITGA3 expression with drug sensitivity in the NCI-60 cancer cell lines [23]. A higher Z score (GI 50) equates to a higher sensitivity of cell lines.

2.12. Statistical analyses

The Kruskal-Wallis test (when the data is not normally distributed) or one-way ANOVA (when the data is normally distributed) was utilized to calculate sample data differences (more than two groups). The Wilcoxon rank-sum test was performed to compute the statistical significance of ITGA3 expression differences between tumors and corresponding normal tissues. The prognosis implication of ITGA3 expression regarding OS, DSS, DFI, and PFI was validated using univariate Cox regression analysis and the Kaplan–Meier method (log-rank test). The correlation of ITGA3 with other factors such as TMB, MSI, CNV, methylation, immune cell infiltration levels, and immune checkpoints was accomplished using Spearman's method. Finally, to calculate whether there was statistical significance in ICB-therapy response proportions between high and low ITGA3 expression groups, the Chi-square test or Fisher exact test was conducted. P value < 0.05 was regarded as statistically significant.

3. Results

3.1. Comprehensive landscape of ITGA3 expression in human cancers

The differences in ITGA3 mRNA expression were obvious in both diverse normal tissues and cancer cell lines. The results revealed that ITGA3 expression levels were higher in most cancer cell lines from the CCLE dataset, especially in the central bile duct, nervous system, pancreas, and thyroid (Fig. 1A). As presented in Fig. 1B, the top three ITGA3-enriched tissues of healthy people from the GTEx dataset were blood vessel, followed by lung and thyroid. In general, ITGA3 expression was elevated in cancer cell lines compared to normal tissues. TCGA and GTEx integrated data showed higher ITGA3 expression in 21 cancer types including BLCA, GBM, LIHC, PAAD, SKCM, STAD, etc. On the contrary, ITGA3 was lowly expressed in ACC, BRCA, LUSC, SARC, UCEC, and UCS (Fig. 1C). Results based on CPTAC demonstrated that ITGA3 protein expression was upregulated in HNSC, PAAD, and GBM and downregulated in LIHC, LUAD, and COAD (Fig. 1D). Immunofluorescence images from HPA database showed that ITGA3 was mainly distributed in the plasma membrane of two different cell lines (U-251 and A-431). In addition, ITGA3 was also distributed in vesicles in the U-251 cell line, and single-cell variation in the staining pattern was observed (Fig. 1E). Based on ComPPI database, we found that cell membrane, extracellular, membrane, mitochondria, nucleus, and secretory pathways were the main distributions of proteins interacting with ITGA3 (Fig. 1F). We further used IHC staining to validate the differential expression of ITGA3 protein. ITGA3 showed medium staining in the liver and lung and high staining in the colon but was not detected in LIHC, LUAD, and COAD. On the contrary, ITGA3 showed high staining in PAAD but was not detected in the pancreas. The results were consistent with our analysis based on CPTAC database. (Fig. 1G).

3.2. ITGA3 gene is correlated with cancerous genomic alteration and methylation

To explore the cause of aberrant ITGA3 expression, we conducted genomic alteration analysis. Incorporating structural variant, mutation, and copy number alteration (CNA) data of cancers, we found that "Mutation" and "Amplification" were the most common alteration types in cancers, and the top three cancer types of alteration frequency (>6 %) were BRCA, UCS, and MESO (Fig. 2A). As well-known tumor immunotherapy predictive biomarkers TMB and MSI could affect the prognosis and therapeutic response of cancer patients [24,25], we evaluated the association of TMB and MSI with ITGA3. The results indicated that ITGA3 was positively correlated with TMB in 4 cancers (ESCA, LAML, PAAD, and THYM) and with MSI in 5 cancers (COAD, KIRC, LUSC, TGCT, and UVM). By contrast, it was negatively correlated with TMB in 6 cancers (ACC, BLCA, BRCA, HNSC, LIHC, and PRAD) and with MSI only in BRCA and PRAD (Fig. 2B and C). As displayed in Fig. 2D, ITGA3 CNV was strongly associated with ITGA3 mRNA expression in most cancer types, scatter plots of the top six correlation scores were presented in Fig. 2E (ACC, BRCA, MESO, OV, STAD, and TGCT, respectively), and it is worth noting that all results are positively correlated. Meanwhile, ITGA3 methylation (β value) was negatively correlated with ITGA3 mRNA expression in various cancers (Fig. 2F). Fig. 2G displays the top six scatter plots with high correlation scores (THYM, ACC, GBM, OV, PAAD, and PRAD, respectively). The methylated CpG islands most associated with ITGA3 expression in each cancer type are presented in Table S3. The univariate Cox regression analysis of four CpG islands (cg10488476, cg12127162, cg14737977, cg26184501) in 25

types of cancer were shown in Fig. S1A. Corresponding to Cox regression analysis, we found that the increased methylation β values of the ITGA3-Body-S_Shore-cg14737977 site in ACC (HR = 4.514 [95 % CI, 1.072–18.996], P = 0.0011) and the ITGA3-Body-Open_Sea-cg26184501 site in BLCA (HR = 1.711 [95 % CI, 1.162–2.52], P = 0.0015) and ESCA (HR = 1.904 [95 % CI, 1.199–3.023], P = 0.0055) reflected a worse OS of patients (Figs. S1B–D). On the contrary, the increased methylation β values of the ITGA3-1stExon; 5′UTR-Island-cg10488476 site in LAML (HR = 0.555 [95 % CI, 0.339–0.908], P = 0.0013) and the ITGA3-Body-Open_Sea-cg26184501 site in KICH (HR = 0.21 [95 % CI, 0.056–0.786], P = 0.023), LGG (HR = 0.364 [95 % CI, 0.252–0.527], P < 0.0001), PAAD (HR = 0.425 [95 % CI, 0.245–0.738], P = 0.00085), and UCEC (HR = 0.47 [95 % CI, 0.293–0.751], P = 0.00034) reflected a better OS of patients (Figs. S1E–I).

3.3. *Prognosis implication of ITGA3 in human cancers*

In this analysis, we validated the clinical prognosis implication of ITGA3. As presented in Fig. 3A, ITGA3 showed prominent prognostic value in various cancer types except PCPG, PRAD, SKCM, UCS, and UVM. Especially, ITGA3 is a risk factor for CESC, HNSC, LUSC, MESO, PAAD, and STAD in all four outcome measures (OS, DSS, DFI, and PFI), indicating that patients with high expression of ITGA3 in the above cancers have a poor prognosis. Moreover, ITGA3 is a protective factor that improves prognosis in patients diagnosed with ACC, BLCA, BRCA, KIRP, and SARC.

The univariate Cox regression analysis of OS revealed that low ITGA3 expression had a significant association with OS prolongation in a variety of tumors. A forest plot was performed in Fig. 3B, demonstrating that low expression of ITGA3 could predict better OS in LGG (HR = 1.975 [95 % CI, 1.637–2.384], P < 0.001), PAAD (HR = 1.456 [95 % Cl, 1.195–1.774], P < 0.001), GBM (HR = 1.306 [95

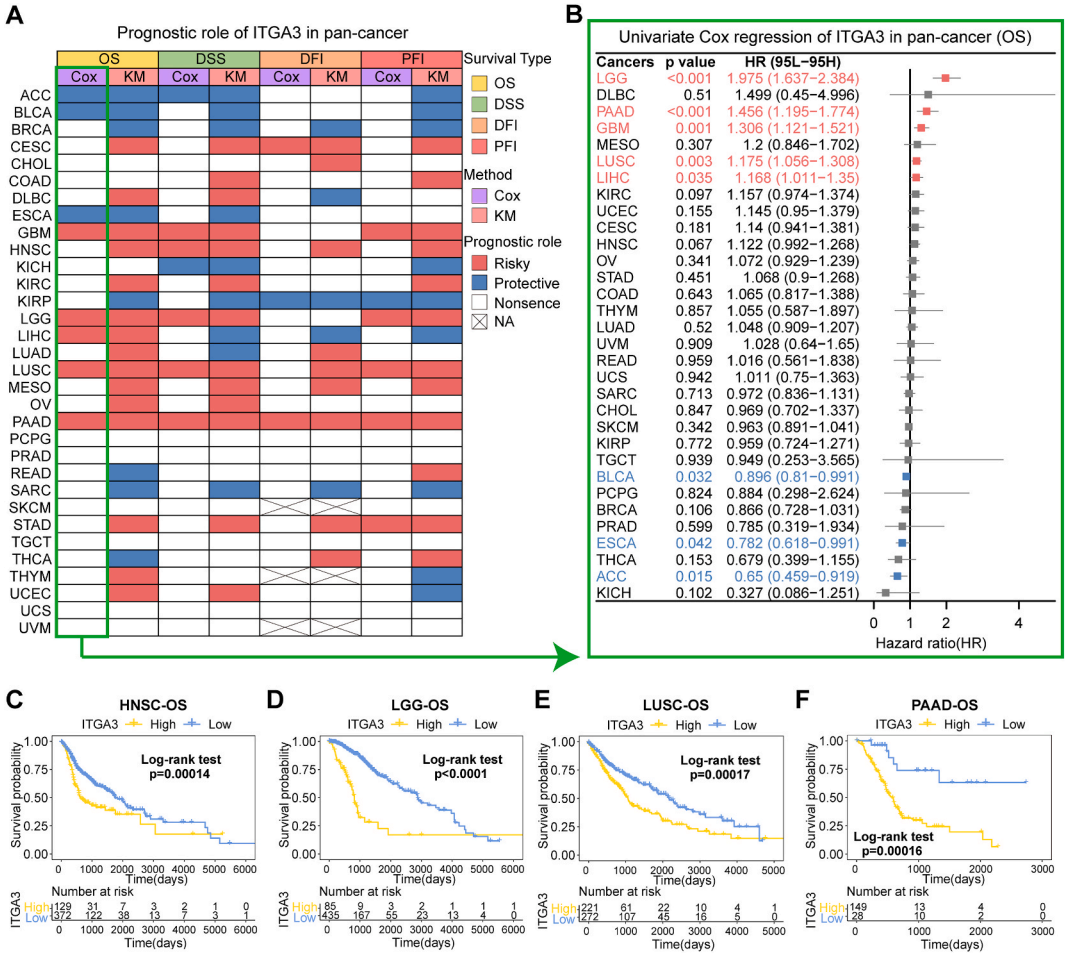

Fig. 3. Prognosis implication of ITGA3 in human cancer. (A) The heatmap base on univariate Cox regression and Kaplan-Meier models summarizes the ITGA3's prognostic role in pan-cancer with four survival type (OS, DSS, DFI, and PFI). The red represents the risk role in the prognosis of cancer patients and the blue represents the protective role in the prognosis of cancer patients. Only p-values <0.05 are shown. (B) The univariate Cox regression analysis of OS illustrated by the forest plot reveals the prognosis implication of ITGA3. The hazard ratio (HR) is a relative prognostic measure of patients. Cancer types highlighted in red indicate ITGA3 as a significant risk factor, while those highlighted in blue indicated ITGA3 as a protective factor. (C–F) Kaplan-Meier OS curves of ITGA3 in HNSC (C), LGG (D), LUSC (E) and PAAD (F).

% Cl, 1.121–1.521], P = 0.001), LUSC (HR = 1.175 [95 % Cl, 1.056–1.308], P = 0.003), LIHC (HR = 1.168 [95 % Cl, 1.011–1.35], P = 0.035), as well as overexpression of ITGA3 could predict time delay of OS in BLCA (HR = 0.896 [95 % Cl, 0.81–0.991], P = 0.032), ESCA (HR = 0.782 [95 % Cl, 0.618–0.991], P = 0.042), ACC (HR = 0.65 [95 % Cl, 0.459–0.919], P = 0.015). In addition, we further conducted Kaplan-Meier curves analysis, four cancers with the most significant results using the log-rank test statistical method were HNSC, LGG, LUSC, and PAAD, all indicating that higher ITGA3 expression was related to poor OS prognosis (Fig. 3C–F).

3.4. GSEA of ITGA3 in pan-cancer

To ascertain the underlying pathway mechanisms of ITGA3, based on the DEGs of the two subgroups with the highest and lowest 30 % of ITGA3 expression, the GSEA of hallmark gene sets was implemented. Our results indicated that immune-related pathways

Fig. 4. Gene set enrichment analysis (GSEA) of ITGA3 in pan-caner. The bubble plot displays the result of the ITGA3 GESA of the hallmarks gene set in pan-cancer. The circle size represents the false discovery rate (FDR) value, and the circle color represents the normalized enrichment score (NES) value. The level of statistical significance is shown through the FDR value, and the NES value reflects the rank of gene classes in the database.

including TNF-α-signaling-via–NF–κB, IFN-γ response, IFN-α response, inflammatory response, IL6-JAK-STAT3 signaling pathway, complement activation regulation, and allograft-rejection pathways, were remarkably enriched in most cancers, especially in ACC, BLCA, CESC, GBM, HNSC, LGG, LUSC, UCEC, and UCS. These results demonstrated that ITGA3 was significantly correlated with immune response processes. It is worth noting that high ITGA3 expression was strongly related to epithelial-mesenchymal transition (EMT) in most cancers, suggesting that high ITGA3 expression may promote invasive and metastatic properties of cancers through EMT. Activated KRAS signaling pathways are prevalent in cancer and could lead to the proliferation, differentiation, and apoptosis of cancer cells [26]. We also found that KRAS signaling pathways are enriched in the high-ITGA3 subgroup, revealing the potential biological role of ITGA3. Furthermore, P53 pathways, apoptosis, blood coagulation cascade, and apical junction also enriched in high-ITGA3 subgroups in various cancers (Fig. 4). In conclusion, GSEA hallmark analysis suggested that ITGA3 was aberrantly

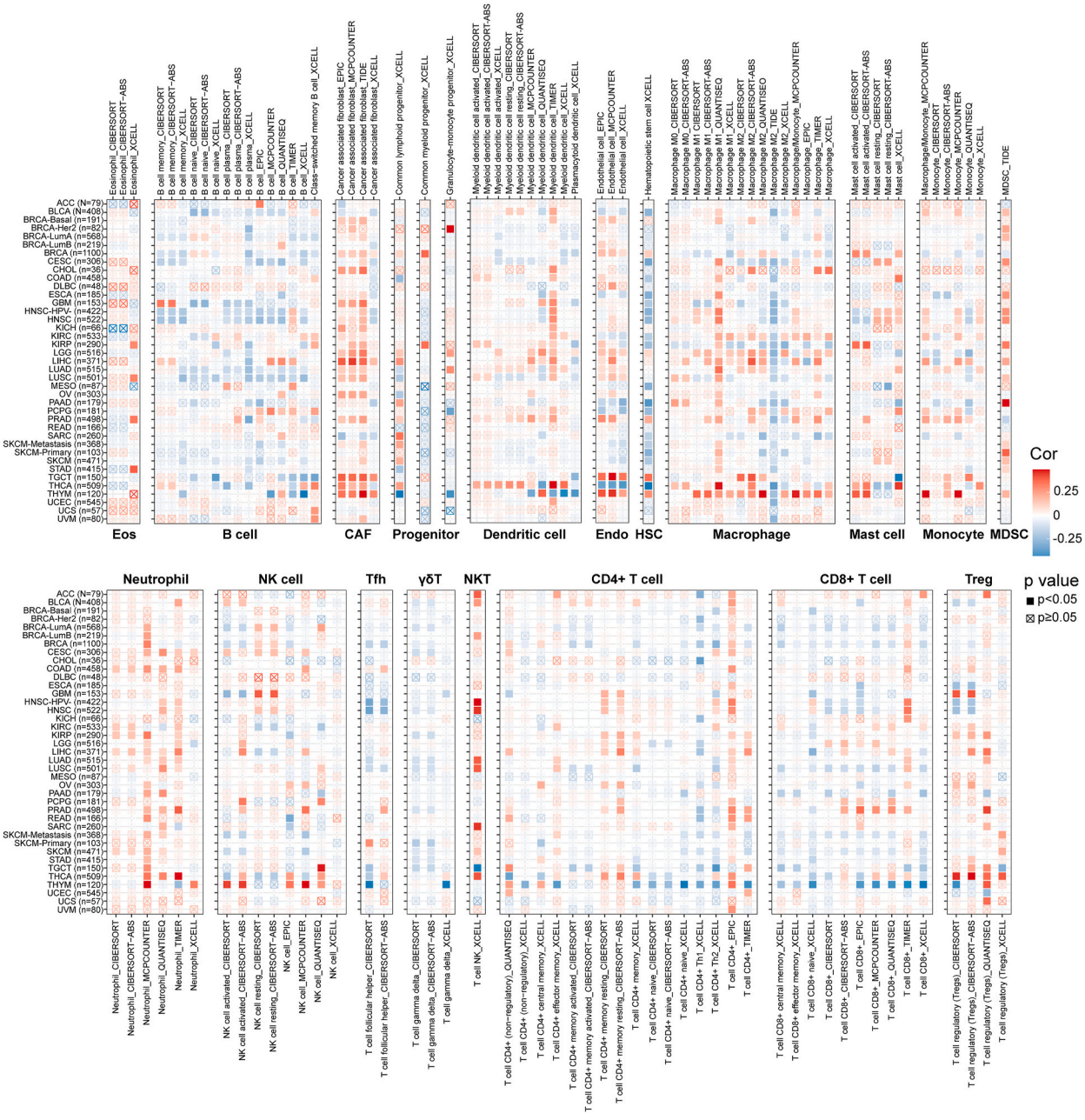

Fig. 5. ITGA3 is involved in immune cell infiltration across human cancers. The heatmap illustrates the correlations of ITGA3 expression and the infiltration levels of Eos, B cell, CAF, progenitor, dendritic cell, Endo, HSC, macrophage, mast cell, monocyte, MDSC, neutrophil, NK cell, Tfh, γδT, NKT, $CD4^+$ T cell, $CD8^+$ T cell, and Treg in pan-cancer. The red square represents the positive correlation and the blue square represents the negative correlation.

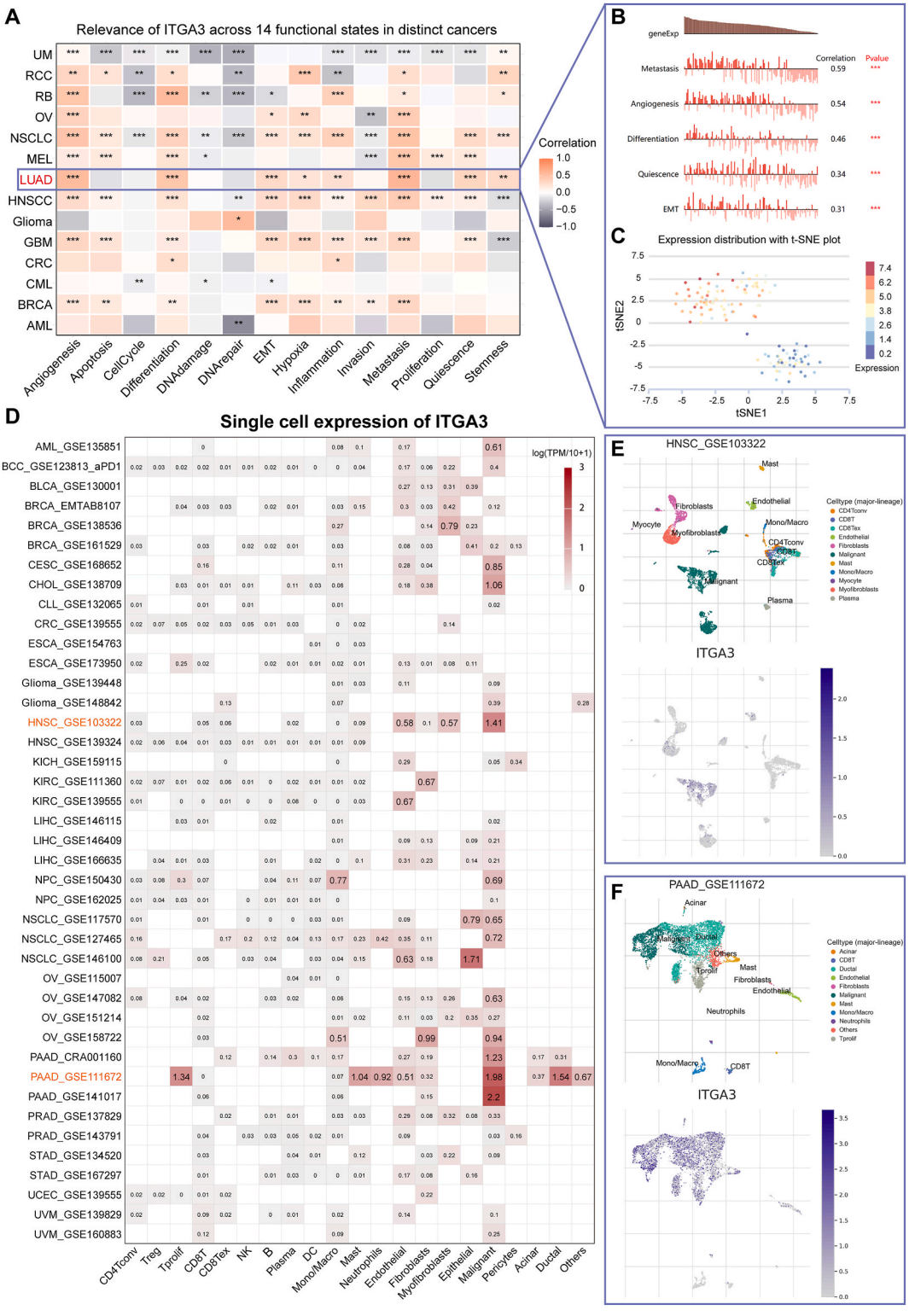

(caption on next page)

Fig. 6. Exploration for functional state and distribution of ITGA3 at single-cell level. (A) Heatmap of the associations of ITGA3 with 14 biology-related functional states in diverse cancer types at a single-cell resolution based on CancerSEA Portal. (B) ITGA3-related functional states in LUAD-EXP0066, which is filtered by correlation strength 0.3. (C) The T-SNE plot describes the ITGA3 expression distribution of cells in LUAD-EXP0066. (D) The heatmap displays a comprehensive landscape of ITGA3 expression levels quantificationally in immune, stromal, and malignant cells. (E) The distribution of ITGA3 in HNSC based on the GSE103322 database. (F) The distribution of ITGA3 in PAAD based on the GSE111672 database. (*p < 0.05, **p < 0.01, ***p < 0.001).

expressed in cancers leading to the related-immune pathways change.

3.5. ITGA3 is involved in immune infiltration across cancers

Based on TIMER2.0 database, we performed immune cell infiltration analysis, ITGA3's positive correlations with the infiltration levels of immune cells including CAFs, macrophages, mast cells, MDSCs, Neutrophils, NKT, and Tregs in the TME, were observed in various cancers, especially in HNSC, LIHC, LUAD, TGCT, THCA, and THYM. In contrast, we found that ITGA3 expression was negatively correlated with the infiltration levels of B cells, HSCs, Tfh, and CD8 T cells across most cancers (Fig. 5). Moreover, we used the

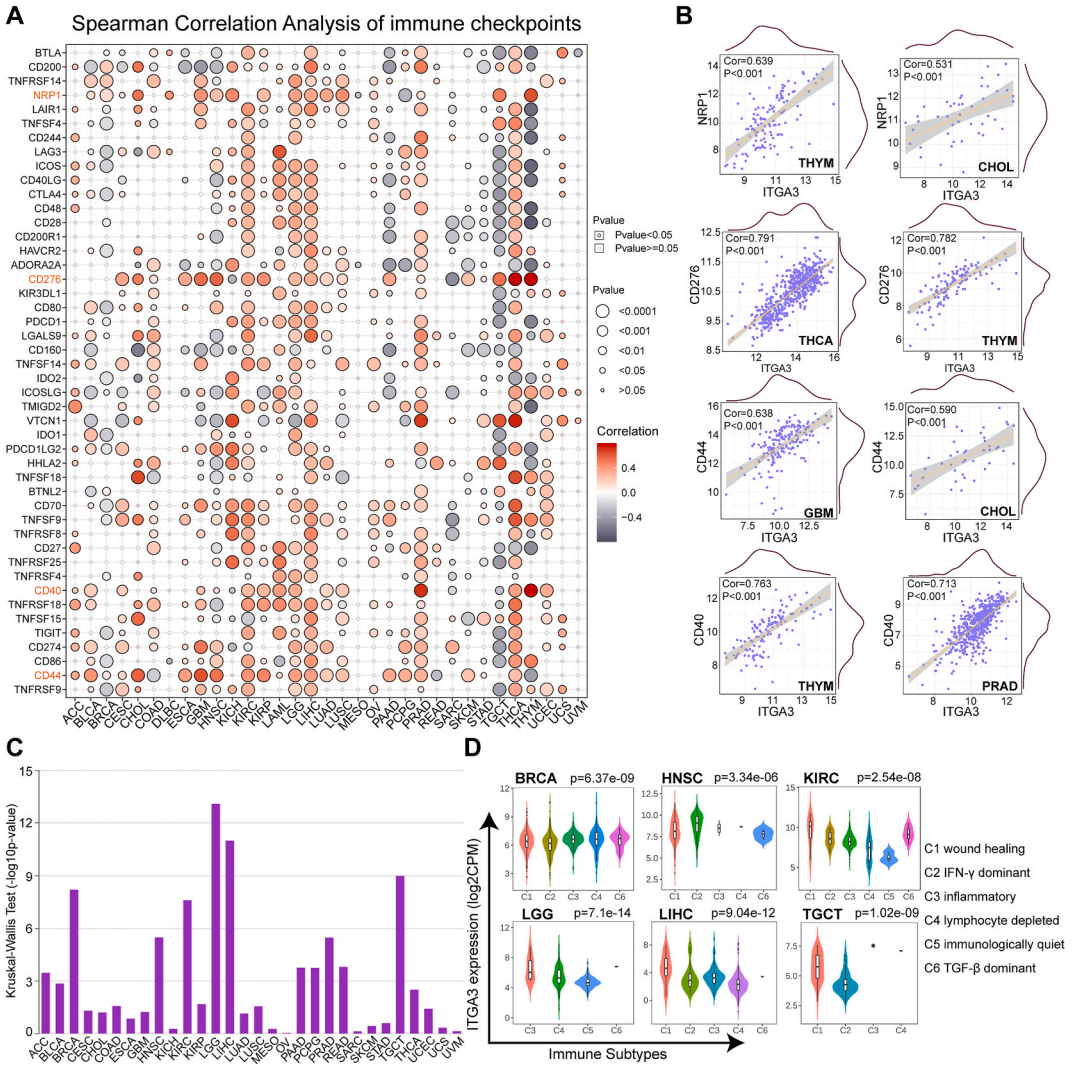

Fig. 7. ITGA3 is associated with immune checkpoints and immune subtypes in pan-cancer. (A) Bubble plot showing the spearman correlations of ITGA3 with immune checkpoints. The circle size reflects the size of the p-value, and the circle color represents the spearman correlation (red positive, grey negative). (B) The scatter plots of the correlation between the four immune checkpoints (NRP1, CD276, CD44, and CD40) and ITGA3 in highly related cancer types. (C) The correlations between ITGA3 and immune subtypes (wound healing, IFN-γ dominant, Inflammatory, lymphocyte depleted, immunologically quiet, or TGF-β dominant) in human cancers based on TSIDB web tool. (D) The expression of ITGA3 in immune subtypes of 6 cancer types (BRCA, HNSC, KIRC, LGG, LIHC, and TGCT).

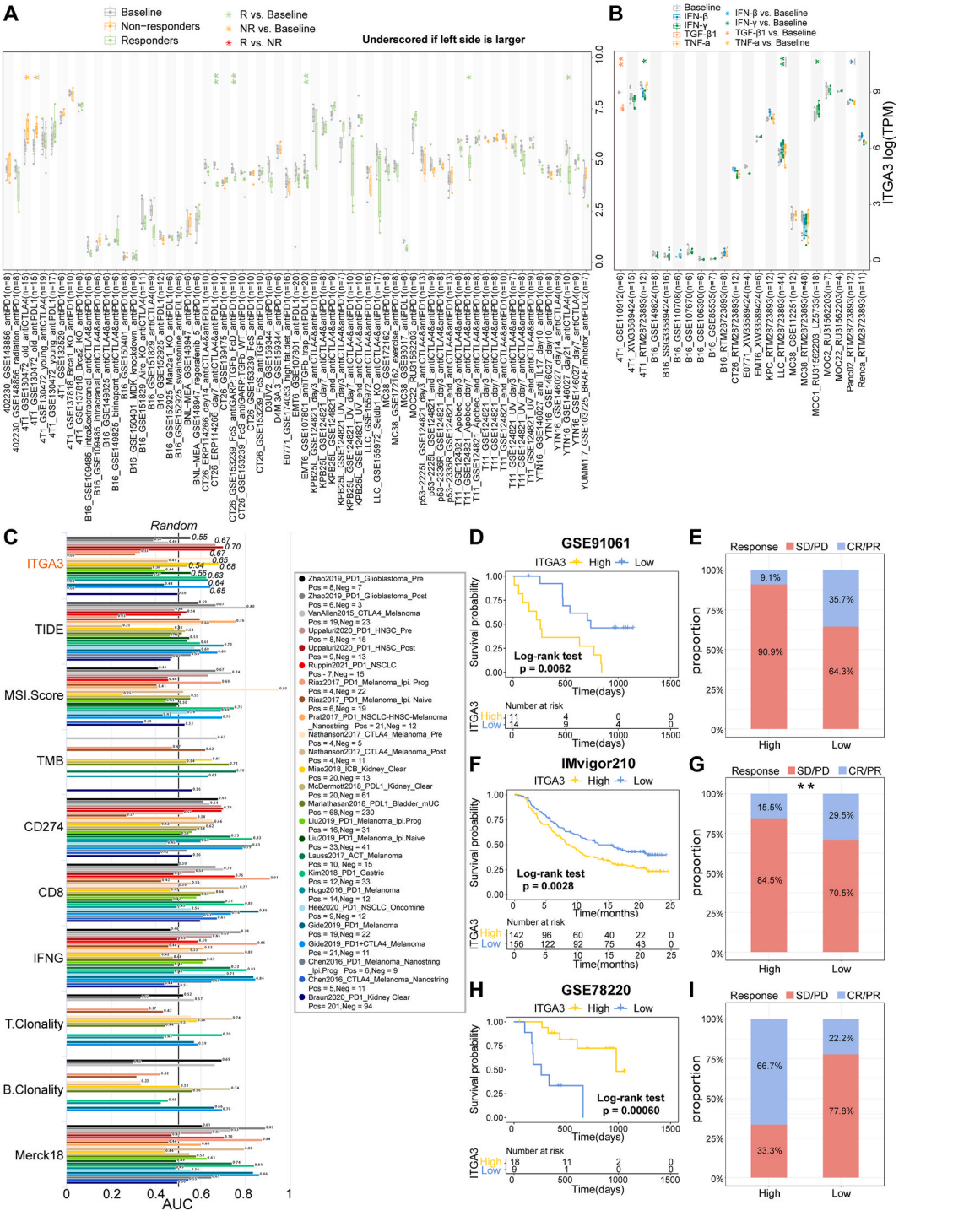

(caption on next page)

Fig. 8. ITGA3 predicts cancer immunotherapy response. (A) ITGA3 expression levels in distinct tumor models and ICB treatments, both pre- and post-ICB intervention, as well as between responders and non-responders. The comparison results between groups are summarized in box plots (underscored if the left side is larger). (B) ITGA3 expression levels between pre- and post-cytokine treated samples across cell lines. The comparison results between groups are summarized in box plots (underscored if left side is larger). (C) A comparison of ITGA3's predictive power of response outcome with other existing biomarkers was applied using the "Biomarker Evaluation " module of TIDE, showing bar plots. AUC was used as a performance indicator to measure the predictive power of biomarkers, a larger AUC (range 0.5–1.0) reflected a better prediction. (D) Kaplan–Meier survival curve of the high- and low-ITGA3 expression patient groups in GSE91061. (E) The response proportion of patients in the low- and high-ITGA3 expression groups in GSE91061. (F) Kaplan–Meier survival curve of the high- and low- ITGA3 expression patient groups in IMvigor210 cohort. (G) The response proportion of patients in the low- and high-ITGA3 expression groups in the IMvigor210 cohort. (H) Kaplan–Meier survival curve of the high- and low-ITGA3 expression patient groups in GSE78220. (I) The response proportion of patients in the low- and high-ITGA3 expression groups in GSE78220. The labeled asterisk indicates the statistical p-value (*$p < 0.05$, **$p < 0.01$, ***$p < 0.001$).

web-based tool CAMOIP to conduct five immune scores (Intratumor Heterogeneity, Macrophage Regulation, Lymphocyte Infiltration Signature Score, TGF-β Response, and Stromal Fraction) of low- and high-ITGA3 expression groups in pan-cancer, the analysis pointed out ITGA3 expression was highly associated with these immune scores, especially in BRCA, HNSC, KIRC, LGG, LIHC, LUSC, PRAD, SARC, TGCT, THCA, THYM, and UCEC (Fig. S2). The differences in TGF-β response scores were eminently observed in all the above cancers.

3.6. Exploration for functional state and distribution of ITGA3 at single-cell level

To clarify the potential function of ITGA3 and distribution of ITGA3 expression in single cells, we estimated the associations of ITGA3 with 14 biology-related functional states in diverse cancer types at a single-cell resolution based on CancerSEA web portal, which indicated that ITGA3 expression was positively associated with functions such as angiogenesis, differentiation, hypoxia and metastasis in RCC-EXP0064, RB-EXP0073, NSCLC-EXP0068, MEL-EXP0071, LUAD-EXP0066, HNSCC-EXP0063, GBM-EXP0057, and BRCA-EXP0052, but showed an inverse association with DNA repair in most cancers (Fig. 6A). As shown in Figs. 6B and 5 functional states are significantly related to ITGA3 in LUAD-EXP0066, which was filtered by correlation strength 0.3. The result indicated that metastasis obtained the highest correlation (cor = 0.59), followed by angiogenesis (cor = 0.54), differentiation (cor = 0.46), quiescence (cor = 0.34), and EMT (cor = 0.31). Additionally, the T-SNE plot described the ITGA3 expression distribution of cells, indicating heterogeneity of expression in two different cell groups (Fig. 6C). Furthermore, we also noticed higher ITGA3 expression levels in malignant and stromal cells than other cell types in cancer datasets representatively using the TISCH2 (Fig. 6D). Pointedly, in the GSE103322 dataset (5902 cells from 18 HNSC patients), ITGA3 was prominently expressed across endothelial, myofibroblasts, and malignant cells (Fig. 6E). Based on the analysis of the GSE111672 dataset (6122 cells from three PAAD patients), ITGA3 highly expressed cell types in the PAAD microenvironment were tprolif, mast, neutrophils, and malignant cells (Fig. 6F).

3.7. ITGA3 is associated with immune checkpoints and immune subtypes

To explore the effects of ITGA3 in immune response, we included commonly recognized immune checkpoints to ascertain ITGA3-related immune checkpoints in the context of ITGA3 expression utilizing Spearman's method. As presented in Fig. 7A we discovered that several immune checkpoints was positively associated with ITGA3 in human cancers, such as NRP1, CD276, CD40, and CD44. Focusing on cancers, we found that in several cancer types, ITGA3 showed a positive correlation with immune checkpoints, such as KICH, KIRC, LGG, LIHC, PRAD, and THCA. The results above suggested ITGA3's efficacy in ICB therapy. Fig. 7B shows the scatter plots of the correlation between the above four immune checkpoints and ITGA3 in highly related cancer types. In addition, we also discovered that ITGA3 was differentially expressed in immune subtypes of 16 cancer types based on TISIDB database (Fig. 7C), the top six results of cancers were shown in Fig. 7D, including BRCA, HNSC, KIRC, LGG, LIHC, and TGCT.

3.8. ITGA3 could predict cancer immunotherapy response

To explore ITGA3's predictive role in cancer immunotherapy response, we used the TIMSO database to perform analysis. Decreased ITGA3 expression levels in vivo across different tumor models and ICB treatments were observed in responders of tumor models including CT26 (anti-CTLA4 + anti-PDL1, anti-PD1, respectively), EMT6 (anti-PDL1), T11 (anti-CTLA4 + anti-PD1), and YTN16 (anti-PD1). Furthermore, increased ITGA3 expression levels were observed in non-responders of tumor model 4T1 (anti-CTLA4, and anti-PDL1, respectively) (Fig. 8A). We also explored ITGA3 expression levels in vitro across cell lines with cytokine treatment, indicating that IFN-γ could up-regulate ITGA3 expression in cell lines MOC1 and LCC, but down-regulate in B16. Meanwhile, TGF-β1 could down-regulate ITGA3 expression in 4T1 cells, IFN-β could up-regulate ITGA3 expression in Panc 02 cells, and TNF-α treatment had no significant effect (Fig. 8B).

We also observed the ITGA's predictive power of response outcomes in immunotherapy, comparison concluded that ITGA3 had a higher predictive value of response outcome (AUC value > 0.5 in 11 immunotherapy cohorts) than existing biomarkers including TMB, T. Clonality, and B.Clonality (AUC values > 0.5 in 8, 7, and 7 in immunotherapy cohorts, respectively), but inferior to TIDE, MSI score, CD274, CD8, IFN-γ, and Merck 18 (Fig. 8C). Subsequently, we found that patients with high ITGA3 expression had lower survival rates and shorter OS time in GSE91061 (25 melanoma patients during immunotherapy with Nivolumab), the anti-PD1 treatment response rate was 26.6 % lower in the group of patients with high ITGA3 expression compared to those with low ITGA3 expression. (Fig. 8D and

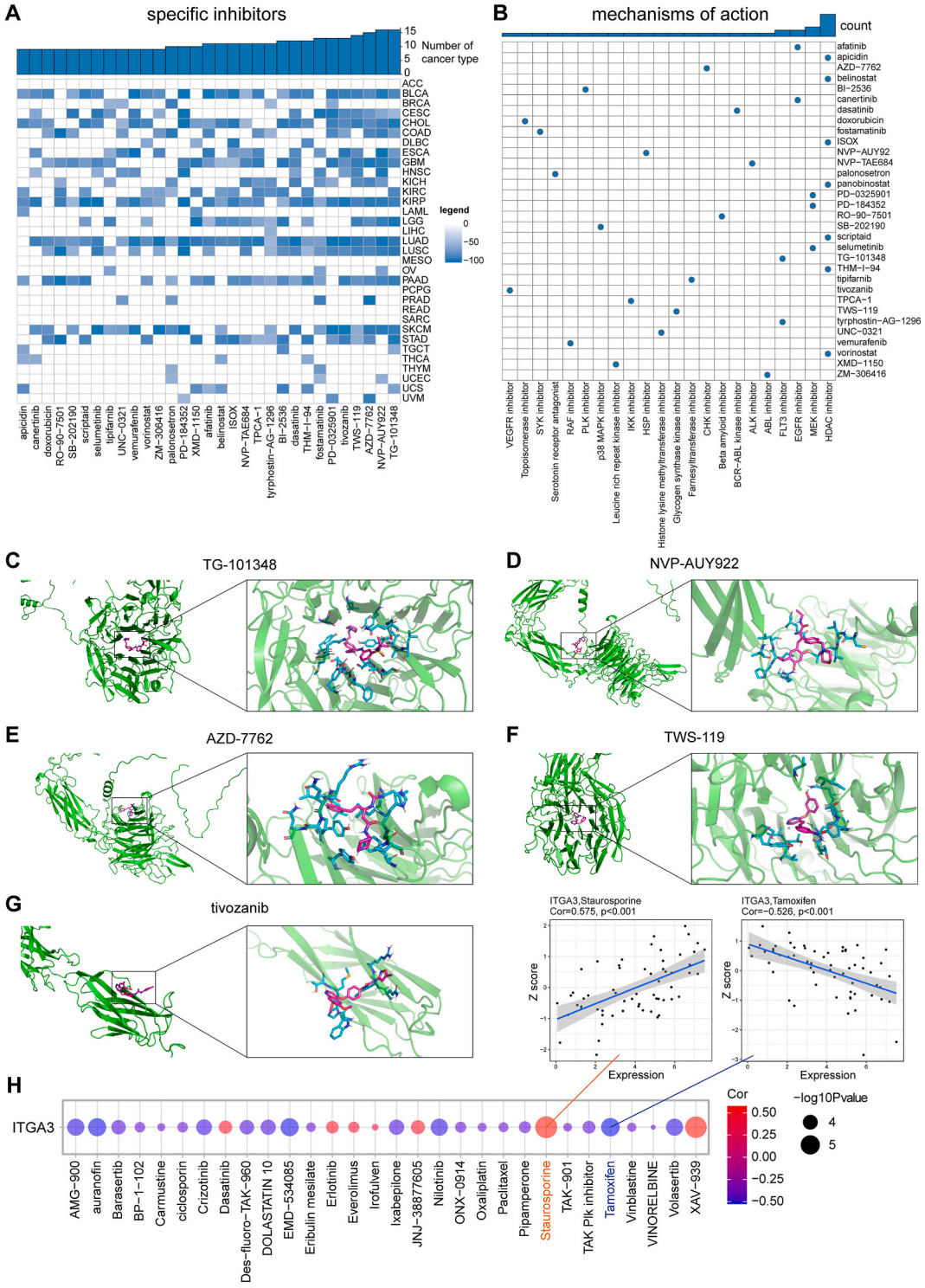

Fig. 9. Compounds targeting ITGA3 prediction and drug sensitivity analysis in pan-cancer. (A) The heatmap exhibits the potential specific inhibitors of ITGA3 enriched in more than 8 types of cancer. The darker the blue, the more negative the CMap score of the specific inhibitors. (B) The scatter plot depicts the mechanisms of action of specific inhibitors. (C–G) Molecular docking results of ITGA3 protein with five compound inhibitors. (H) Heatmap of the association of ITGA3 expression with drug sensitivity (Z-score) in the NCI-60 cancerous cell lines. Scatter plots of the drugs with the highest correlation score (positive or negative) are shown.

E). IMvigor210 cohort (298 metastatic urothelial cancer patients receiving anti-PD-L1 agent atezolizumab) showed the same trend in our research, whose proportion reached 14 % (Fig. 8F and G). Conversely, in the GSE78220 cohort (27 patients undergoing anti-PD1 therapy in metastatic melanoma), patients with high expression of ITGA3 had a longer OS time and a 44.5 % lower non-response rate to anti-PD1 treatment than the low ITGA3 expression group (Fig. 8H and I). The above analysis suggested ITGA3's potential role in predicting cancer immunotherapy response.

3.9. ITGA3 targeted inhibitors screening and drug sensitivity analysis in human cancers

Finally, to further explore ITGA3's promising value, targeted compound inhibitors screening and drug analysis were entered into our study. As shown in Fig. 9A, TG-101348 is the compound that involved the most numbers of cancer types, followed by NVP-AUY922, AZD-7762, TWS-119, tivozanib, etc., which showed strong potential to target ITGA3. Notably, we found no compounds enriched in ACC, MESO, PCPG, READ, and SARC. We also explored the mechanisms of action of these compounds and found that most belong to HDAC inhibitors, followed by MEK inhibitors (Fig. 9B). Furthermore, to test the targeting ITGA3 potential of compounds, we performed molecular docking. Molecular docking results of ITGA3 protein with the 5 compounds were shown. TG-101348 could effectively bind ITGA3, whose docking energies are −7.41 (kcal/mol) (Fig. 9C). Molecular docking also showed binding energies of NVP-AUY922 (−4.96 kcal/mol) (Fig. 9D), AZD-7762 (−4.74 kcal/mol) (Fig. 9E), TWS-119 (−6.13 kcal/mol) (Fig. 9F), and tivozanib (−5.33 kcal/mol) (Fig. 9G). The results of the drug sensitivity analysis are presented in Fig. 9H. We screened 30 drugs whose sensitivity was significantly correlated with ITGA3 expression ($p < 0.001$). Scatter plots displayed that the drugs with the highest correlation score (positive or negative) were staurosporine and tamoxifen, respectively.

4. Discussion

Immunotherapy, as an emerging and promising treatment modality, has brought revolutionary changes to cancer treatment. ICB therapy (targeting PD-1/PD-L1 and CTLA-4, etc.) has achieved promising results in human cancer [27]. Nevertheless, most cancer patients still have poor curative effects and poor prognoses on ICB therapy, finding new potential therapeutic targets and in-depth exploration of the mechanisms affecting immunotherapy are still problems that need to be resolved.

ITGA3, as a member of the integrin alpha chain family, is a surface adhesion molecule that acts in the ECM and is involved in many steps of cancer progression, especially in promoting cancer invasion, proliferation, apoptosis, and metastasis [11,28,29]. In addition, ITGA3 was confirmed to stimulate the migratory and invasive properties of breast cancer cells through interaction with VASP to regulate its expression, and the activity of the PI3K-AKT axis could be inhibited by the downregulation of ITGA3 [30]. Shirakihara et al. concluded that ITGA3 is positively regulated by the δEF-1 and MEK-ERK pathways, which is a potential marker protein for cells undergoing enhanced EMT and invasive cancer cells [31]. ITGA3 is also regulated by various microRNAs, especially the microRNA-199 family [10,32]. It is noteworthy that recent studies have proposed several promising mechanisms for integrin-targeted immunotherapy. Targeting integrins could enhance the efficacy of PD-1/PD-L1 inhibitors and inhibit the secretion of TGF-β in the TME, thereby demonstrating significant anti-tumor activity [7,33]. Interestingly, a recent study demonstrated that increased ITGA3 expression is associated with a malignant phenotype in pancreatic cancer, characterized by higher PD-L1 expression and decreased infiltration of $CD8^+$ T cells [34]. However, the potential mechanisms by which ITGA3 in the TME influences tumor development and immune response remain to be further explored. The emergence of various biological information databases has brought a large amount of data and tools for our scientific research on the biological function of ITGA3. A comprehensive pan-cancer analysis of ITGA3 was conducted by us in this study to explore its underlying mechanism. Moreover, we revealed ITGA3 as a potential biomarker of response to immunotherapy and screened out several targeted compound inhibitors of ITGA3.

implications, Firstly, we conducted a multifaceted pan-cancer analysis of ITGA3 at genome, transcriptome, and proteome levels based on various databases. ITGA3 expression levels of mRNA and protein significantly increased in most cancers, and expression differences in corresponding cancers are consistent with several previous studies [35,36]. TMB and MSI have emerged as major response-predictive biomarkers for the effectiveness of ICB therapy [24,25]. CNV, as a form of genomic structural variation, has been proven to be involved in the occurrence and development of various cancers and affects the prognosis of patients [37,38], and can also be used in cancer diagnosis [39]. As an epigenetic modification, DNA methylation often disrupts gene regulation and affects patient prognosis in a variety of cancers [40,41]. Genomic alteration and modification analysis revealed ITGA3 was remarkably related to TMB, MSI, CNV, and DNA methylation in specific cancers, suggesting ITGA3 may be aberrantly expressed and could promote cancer progression and immunotherapy response through the above processes. It is worth mentioning that we identified several CpG islands (cg10488476, cg14737977, cg26184501) that have a significant influence on the mRNA expression of ITGA3 and have prognosis implication. Among them cg26184501 could reflect better or worse OS of patients in various cancers. Furthermore, our analysis of OS prognostics based on ITGA3 methylation has revealed results that are opposite to those based on ITGA3 transcript levels, thus validating our findings to a certain extent. These findings provide valuable insights into the potential of CpG islands in regulating ITGA3 expression and their impact on cancer prognosis.

Next, we explore the predictive prognosis implication of ITGA3 in cancer patients. Based on four outcome measures (OS, DSS, DFI, and PFI, respectively), Cox regression and Kaplan–Meier analysis revealed a dual role for ITGA3 as a protective factor in 7 cancer types and a risk factor in 12 cancer types. Analysis suggested that ITGA3 is a promising prognostic predictor in cancers, some results could be corroborated by previous studies [9,36,42].

Then we conducted GSEA, suggesting ITGA3 was strongly relevant to immune-related pathways, including TNF-α-signaling-via–NF–κB, IFN-γ response, IFN-α response, inflammatory response, IL6-JAK-STAT3 signaling pathway, complement activation

regulation, allograft-rejection pathways. In recent studies, these immune responses or pathways have been shown to influence the efficacy of tumor immunotherapy. Sun et al. found that LRRK2 acted as an immunosuppressive gene and was upregulated by $CD8^+$ T cells via IFN-γ to affect cancer immunotherapy efficacy [43]. Sorrentino et al. reported that SIK3 regulates tumor resistance to cytotoxic T-cell attacks by activating pro-survival and anti-apoptotic genes through the NF-κB pathway, protecting against TNF-induced cytotoxicity [44]. The result of GSEA suggests that ITGA3 may interact with related cytokines in the ECM during these immune response pathways to participate in cancer progression and immunotherapy response.

The TME, comprising immune cells, stromal cells, cytokines, and ECM, has been demonstrated to exert a crucial influence on cancer progression, while also limiting the efficacy of immunotherapy and imposing formidable obstacles to cancer treatment [27,45]. CAFs are important components of the TME. Activated CAFs could promote angiogenesis, cancer progression, invasion, and metastasis, and cause ECM remodeling [46]. Moreover, as vital surface adhesion receptors mediate interactions between the ECM, the regulation of integrins in the ECM may be closely related to the above processes [4]. In addition, previous studies have found that Tregs and MDSCs could help tumors avoid the response to immunotherapy and promote tumor immunosuppression [47–50]. Activated TGF-β could lead to the formation of EMT and CAFs, and simultaneously cause the dysregulation of genes in the ECM, which ultimately affects the efficacy of immunotherapy [51,52]. To reveal the potential mechanism of ITGA3 in the TME, we conducted immune cell infiltration analysis and found that ITGA3 had positively correlated with CAFs, Neutrophils, MDSCs, and Tregs in most cancers. We also found that patients of most cancers with high expression of ITGA3 had higher TGF-β scores. A small number of cancers showed the opposite results, suggesting that ITGA3 could play different roles in different cancer types. In addition, the results based on single-cell analysis revealed that ITGA3 plays a variety of roles in shaping the TME and promoting cancer development, such as angiogenesis, differentiation, hypoxia, and metastasis. Notably, combining antiangiogenic therapies and immunotherapies might increase the effectiveness of immunotherapy [53], thus further exploration of the mechanism of ITGA3 in angiogenesis could provide strategies for enhancing the efficacy of immunotherapy. The above results revealed ITGA3's vital role in TME. It may regulate the infiltration levels of various cells through TGF-β response to affect tumor immunity and immunotherapy response. The strategy for targeted modulation of ITGA3 may be able to have a positive effect on anti-tumor immunotherapy.

In this study, we also uncovered ITGA3's positive association with specific ICPs in cancers, especially NRP1 and CD276. CD271 and NRP1 are vital negative immunomodulators in TME, and the immunotherapy regimens targeting CD276 and NRP1 have shown great promise [54,55]. Based on these results, studying the potential mechanism of ITGA3 with CD276 and RNP1 will help to optimize related cancer immunotherapy further. In addition, CD44 also showed a positive correlation with ITGA3. Many recent studies point to the role of CD44 in cancer progression and tumor immunity, as a molecular marker of CSCs, CD44 could promote tumorigenesis and has the therapeutic potential to be a molecular target in cancer therapy [56–58]. ITGA3 also acts as a cell surface molecule, which may be mechanically associated with CD44. Subsequently, we revealed the ITGA3's predictive value in immunotherapy response. Based on the data from mouse samples with ICB and cytokines treatment, we found that the responders treated with ICB showed lower expression of ITGA3, while non-responders showed the opposite. Moreover, tumor lines treated with cytokines showed that IFN-γ could significantly down-regulate ITGA3 expression levels in cancer cell lines. Combined with the trend of ICB therapy in vivo, we concluded that IFN-γ may be an effective cytokine targeting ITGA3 to increase the immunotherapy response rate. Of course, the situation may be different in humans, which requires further research and exploration. Biomarker evaluation based on immunotherapy cohorts showed that ITGA3 alone had an AUC >0.5 in 11 immunotherapy cohorts, indicating ITGA3's predictive power of immunotherapy response. Benefiting from a growing number of published immunotherapy cohort studies, we also discovered melanoma patients (GSE91061) with high ITGA3 expression under anti-PD1 treatment had a poor prognosis, as did metastatic urothelial cancer patients (IMvigor210 cohort) under anti-PDL1 treatment. However, the situation was reversed in another cohort of melanoma patients (GSE78220) treated with anti-PD1, suggesting that the predictive role of ITGA3 was not set in stone and may be influenced by other underlying factors.

Finally, we predicted several potential inhibitors targeting ITGA3 and sensitive drugs. Through screening, we obtained a series of possible specific inhibitors of ITGA3 from the CMap database, such as TG-101348, NVP-AUY922, AZD-7762, TWS-119, tivozanib, etc. In addition, we also performed molecular docking utilizing AutoDock Tools to test the targeting ability of these compounds. It is worth noting that most of the specific inhibitor compounds belong to HDAC inhibitors and MEK inhibitors. A combination of HDAC inhibitors with immunotherapy is a promising cancer treatment strategy [59]. The use of HDAC inhibitors may modulate the effect of ITGA3 on the immunotherapy response. MEK inhibitors could target RAS/RAF/MEK/ERK signaling pathway [26]. Combined with GSEA analysis results, we concluded that ITGA3 may be involved in the above pathway. Correspondingly, previous research clarified the expression of ITGA3 could be downregulated by U0126, a MEK 1/2 inhibitor [31]. In summary, we provided some candidate compounds or drugs for the study of targeting ITGA3 in cancer therapy, whose efficacy needs to be verified by subsequent mechanism studies.

In this study, we conducted a detailed bioinformatic analysis of ITGA3 based on expression profiles, clinical information, and drug data from publicly available databases. Admittedly, although we produced several discoveries, there are some limitations to our analytical methods. We used univariate Cox regression analysis to identify the prognosis implication of ITAG3, which ignores other potential confounding variables that may affect the results. These confounding variables may lead to biases in the effects of risk factors. When screening potential compound inhibitors of ITGA3, our analysis involves three main parts. Firstly, we defined low- and high-ITGA3 subgroups to ascertain DEGs as disease signatures. More reliable disease signatures may exist. Secondly, we obtained the drug signature based on the CMap database. The predictive ability of drug target prediction using Cmap analysis has been partially validated by several studies [60]. Drug signatures from other databases may need to be collected in the future to further validate our results. Lastly, we utilized the Kolmogorov-Smirnov method to calculate the CMap score. However, this method may not be the best computational method for CMap analysis [61]. To address the constraint of limited computing resources, we conducted a preliminary screening of drugs for molecular docking using the CMap score. However, due to the unconfirmed structure of the ITGA3 protein, we

employed the artificial intelligence system AlphaFold to predict its 3D structure based on the amino acid sequence. It is important to acknowledge that this approach may introduce some bias in the results. Furthermore, the efficacy of these potential inhibitors in terms of targeting performance requires further validation in future studies. In addition, most of our research was based on open-source databases, analysis outcomes without large-scale clinical cohorts to confirm, and the mechanism of ITGA3 in tumor immunity needs more cell and animal experiments to clarify.

5. Conclusions

In summary, we performed an integrated analysis of ITGA3 in pan-cancer, our analysis indicated that ITGA3 was aberrantly expressed in multiple cancers and was associated with genomic alteration, methylation, prognosis, immune infiltration, tumor microenvironment, and immunotherapy response, which may be a promising response-predictive biomarker and potential therapeutic target. Considering the above functions of ITGA3, we predicted potential inhibitors targeting ITGA3 and sensitive drugs for future therapeutic strategies.

Declarations

Ethics approval and consent to participate

Not applicable.

Consent for publication

Not applicable.

Availability of data and materials

The datasets presented in this study can be found in online repositories. The names of the repository/repositories and accession number(s) can be found in the article/Supplementary Material.

Competing interests

The authors declare that they have no competing interests.

Funding

The research project is supported by the National Natural Science Foundation (grant nos. 82,273,068, 82,260,524, and 82,172,989), Key Research and Development projects, Jiangxi Province, China (20212BBG73021), Jiangxi Training Program for academic and technical leaders of major disciplines – Young talents program (20212BCJ23023), Key project of Science and Technology Innovation of Health Commission (2023ZD003), Jiangxi Province Department of Education Science and technology research project, China (grant no. GJJ210177)

Data availability statement

Data included in article/suppmaterial/referenced in article.

Additional information

No additional information is available for this paper.

CRediT authorship contribution statement

Jiawei Gui: Writing – original draft, Visualization, Software. **Lufei Yang:** Writing – original draft, Visualization. **Junzhe Liu:** Writing – review & editing, Data curation. **Yishuang Li:** Writing – review & editing. **Mi Zou:** Writing – review & editing. **Chengpeng Sun:** Writing – review & editing. **Le Huang:** Writing – review & editing. **Xingen Zhu:** Supervision, Investigation, Funding acquisition. **Kai Huang:** Supervision, Investigation, Funding acquisition.

Declaration of competing interest

The authors declare that they have no known competing financial interests or personal relationships that could have appeared to influence the work reported in this paper.

Acknowledgments

We sincerely acknowledge the contributions from the TCGA project, GTEx project, and GEO project.

Abbreviations

ITGA3	integrin subunit α3
TME	tumor microenvironment
TIME	tumor immune microenvironment
ECM	extracellular matrix
GSEA	gene set enrichment analysis
CMap	ConnectivityMap
CCLE	Cancer Cell Line Encyclopedia
TCGA	The Cancer Genome Atlas
GTEx	Genotype-Tissue Expression
GEO	Gene Expression Omnibus
HPA	Human Protein Atlas
IHC	Immunohistochemistry
ComPPI	Compartmentalized Protein-Protein Interaction
GSCA	Gene Set Cancer Analysis
TMB	tumor mutational burden
MSI	microsatellite instability
CNA	copy number alteration
CNV	copy number variation
OS	overall survival
DSS	disease-specific survival
DFS	disease-free survival
PFI	progression-free interval
DEGs	Differentially Expressed Genes
NES	Normalized Enrichment Score
FDR	False Discovery Rate
Eos	eosinophil
CAFs	cancer-associated fibroblasts
Endo	endothelial cells
HSCs	hematopoietic stem cells
Tregs	regulatory T cells
ICB	immune checkpoint blockade
EMT	epithelial-mesenchymal transition
ACC	Adrenocortical carcinoma
BLCA	Bladder Urothelial Carcinoma
BRCA	Breast invasive carcinoma
CESC	Cervical squamous cell carcinoma and endocervical adenocarcinoma
CHOL	Cholangiocarcinoma
COAD	Colon adenocarcinoma
DLBC	Lymphoid Neoplasm Diffuse Large B-cell Lymphoma
ESCA	Esophageal carcinoma
GBM	Glioblastoma multiforme
HNSC	Head and Neck squamous cell carcinoma
KICH	Kidney Chromophobe
KIRC	Kidney renal clear cell carcinoma
KIRP	Kidney renal papillary cell carcinoma
LAML	Acute Myeloid Leukemia
LGG	Brain Lower Grade glioma
LIHC	Liver hepatocellular carcinoma
LUAD	Lung adenocarcinoma
LUSC	Lung squamous cell carcinoma
MESO	Mesothelioma
OV	Ovarian serous cystadenocarcinoma
PAAD	Pancreatic adenocarcinoma
PCPG	Pheochromocytoma and Paraganglioma
PRAD	Prostate adenocarcinoma

READ	Rectum adenocarcinoma
SARC	Sarcoma
SKCM	Skin Cutaneous Melanoma
STAD	Stomach adenocarcinoma
TGCT	Testicular Germ Cell Tumors
THCA	Thyroid carcinoma
THYM	Thymoma
UCEC	Uterine Corpus Endometrial Carcinoma
UCS	Uterine Carcinosarcoma
UVM	Uveal Melanoma

Appendix A. Supplementary data

Supplementary data to this article can be found online at https://doi.org/10.1016/j.heliyon.2024.e24236.

References

[1] R.L. Siegel, et al., Cancer statistics, 2022, CA Cancer J Clin 72 (1) (2022) 7–33.
[2] T. Tang, et al., Advantages of targeting the tumor immune microenvironment over blocking immune checkpoint in cancer immunotherapy, Signal Transduct Target Ther 6 (1) (2021) 72.
[3] A. Goenka, et al., Tumor microenvironment signaling and therapeutics in cancer progression, Cancer Commun. 43 (5) (2023) 525–561.
[4] F. Liu, et al., Integrins in cancer: emerging mechanisms and therapeutic opportunities, Pharmacol. Ther. 247 (2023) 108458.
[5] J.D. Humphries, A. Byron, M.J. Humphries, Integrin ligands at a glance, J. Cell Sci. 119 (Pt 19) (2006) 3901–3903.
[6] Q. Zhang, et al., The Interplay between integrins and immune cells as a regulator in cancer immunology, Int. J. Mol. Sci. 24 (7) (2023).
[7] S. Ruan, et al., Integrin β4-targeted cancer immunotherapies inhibit tumor growth and decrease metastasis, Cancer Res. 80 (4) (2020) 771–783.
[8] D.A. Cobb, et al., Targeting of the alpha(v) beta(3) integrin complex by CAR-T cells leads to rapid regression of diffuse intrinsic pontine glioma and glioblastoma, J Immunother Cancer 10 (2) (2022).
[9] A. Wu, et al., Integrated analysis of prognostic and immune associated integrin family in ovarian cancer, Front. Genet. 11 (2020) 705.
[10] L. Tian, et al., MicroRNA-199a-5p suppresses cell proliferation, migration and invasion by targeting ITGA3 in colorectal cancer, Mol. Med. Rep. 22 (3) (2020) 2307–2317.
[11] J. Du, et al., Silencing of integrin subunit α3 inhibits the proliferation, invasion, migration and autophagy of esophageal squamous cell carcinoma cells, Oncol. Lett. 24 (2) (2022) 271.
[12] J. Yao, L. Wang, Integrin α3 mediates stemness and invasion of glioblastoma by regulating POU3F2, Curr. Protein Pept. Sci. 24 (3) (2023) 247–256.
[13] D.S. Chandrashekar, et al., UALCAN: a portal for facilitating tumor subgroup gene expression and survival analyses, Neoplasia 19 (8) (2017) 649–658.
[14] V. Modhukur, et al., MethSurv: a web tool to perform multivariable survival analysis using DNA methylation data, Epigenomics 10 (3) (2018) 277–288.
[15] A. Subramanian, et al., Gene set enrichment analysis: a knowledge-based approach for interpreting genome-wide expression profiles, Proc Natl Acad Sci U S A 102 (43) (2005) 15545–15550.
[16] G. Yu, et al., clusterProfiler: an R package for comparing biological themes among gene clusters, OMICS 16 (5) (2012) 284–287.
[17] A. Lin, et al., CAMOIP: a web server for comprehensive analysis on multi-omics of immunotherapy in pan-cancer, Brief Bioinform 23 (3) (2022).
[18] H. Yuan, et al., CancerSEA: a cancer single-cell state atlas, Nucleic Acids Res. 47 (D1) (2019) D900–d908.
[19] V. Thorsson, et al., The immune landscape of cancer, Immunity 48 (4) (2018) 812–830.e14.
[20] B. Ru, et al., TISIDB: an integrated repository portal for tumor-immune system interactions, Bioinformatics 35 (20) (2019) 4200–4202.
[21] Z. Zeng, et al., TISMO: syngeneic mouse tumor database to model tumor immunity and immunotherapy response, Nucleic Acids Res. 50 (D1) (2022) D1391–d1397.
[22] J. Lamb, The Connectivity Map: a new tool for biomedical research, Nat. Rev. Cancer 7 (1) (2007) 54–60.
[23] U.T. Shankavaram, et al., CellMiner: a relational database and query tool for the NCI-60 cancer cell lines, BMC Genom. 10 (2009) 277.
[24] S.S. Joshi, B.D. Badgwell, Current treatment and recent progress in gastric cancer, CA Cancer J Clin 71 (3) (2021) 264–279.
[25] L.M. Sholl, et al., The promises and challenges of tumor mutation burden as an immunotherapy biomarker: a perspective from the international association for the study of lung cancer pathology committee, J. Thorac. Oncol. 15 (9) (2020) 1409–1424.
[26] J. Han, et al., MEK inhibitors for the treatment of non-small cell lung cancer, J. Hematol. Oncol. 14 (1) (2021) 1.
[27] Y. Zhang, Z. Zhang, The history and advances in cancer immunotherapy: understanding the characteristics of tumor-infiltrating immune cells and their therapeutic implications, Cell. Mol. Immunol. 17 (8) (2020) 807–821.
[28] H. Hamidi, J. Ivaska, Every step of the way: integrins in cancer progression and metastasis, Nat. Rev. Cancer 18 (9) (2018) 533–548.
[29] I.V. Bijnsdorp, et al., Exosomal ITGA3 interferes with non-cancerous prostate cell functions and is increased in urine exosomes of metastatic prostate cancer patients, J. Extracell. Vesicles 2 (2013).
[30] H. Zhang, et al., ITGA3 interacts with VASP to regulate stemness and epithelial-mesenchymal transition of breast cancer cells, Gene 734 (2020) 144396.
[31] T. Shirakihara, et al., Identification of integrin α3 as a molecular marker of cells undergoing epithelial-mesenchymal transition and of cancer cells with aggressive phenotypes, Cancer Sci. 104 (9) (2013) 1189–1197.
[32] K. Koshizuka, et al., Regulation of ITGA3 by the anti-tumor miR-199 family inhibits cancer cell migration and invasion in head and neck cancer, Cancer Sci. 108 (8) (2017) 1681–1692.
[33] F. Liu, et al., Targeting integrin αvβ3 with indomethacin inhibits patient-derived xenograft tumour growth and recurrence in oesophageal squamous cell carcinoma, Clin. Transl. Med. 11 (10) (2021) e548.
[34] X. Zheng, et al., ITGA3 acts as a purity-independent biomarker of both immunotherapy and chemotherapy resistance in pancreatic cancer: bioinformatics and experimental analysis, Funct. Integr. Genomics 23 (2) (2023) 196.
[35] Y. Jiao, et al., ITGA3 serves as a diagnostic and prognostic biomarker for pancreatic cancer, OncoTargets Ther. 12 (2019) 4141–4152.
[36] Y. Li, et al., ITGA3 is associated with immune cell infiltration and serves as a favorable prognostic biomarker for breast cancer, Front. Oncol. 11 (2021) 658547.
[37] J. Carron, et al., Association of inherited copy number variation in ADAM3A and ADAM5 pseudogenes with oropharynx cancer risk and outcome, Genes 13 (12) (2022).
[38] T. Liu, et al., Genome-wide transcriptomics and copy number profiling identify patient-specific CNV-lncRNA-mRNA regulatory triplets in colorectal cancer, Comput. Biol. Med. 153 (2023) 106545.

[39] A. Abou-Zeid, et al., HOXA9 gene promotor methylation and copy number variation of SOX2 and HV2 genes in cell free DNA: a potential diagnostic panel for non-small cell lung cancer, BMC Cancer 23 (1) (2023) 329.
[40] G. Anuraga, et al., Potential prognostic biomarkers of NIMA (never in mitosis, gene A)-Related kinase (NEK) family members in breast cancer, J Pers Med 11 (11) (2021).
[41] C. Xing, et al., Integrate analysis of the promote function of Cell division cycle-associated protein family to pancreatic adenocarcinoma, Int. J. Med. Sci. 18 (3) (2021) 672–684.
[42] J. Zhou, et al., Identification of novel genes associated with a poor prognosis in pancreatic ductal adenocarcinoma via a bioinformatics analysis, Biosci. Rep. 39 (8) (2019).
[43] K. Sun, et al., Targeting leucine-rich repeat serine/threonine-protein kinase 2 sensitizes anti-PD-L1 immunotherapy of pancreatic ductal adenocarcinoma, Mol. Ther. 31 (10) (2023) 2929–2947.
[44] A. Sorrentino, et al., Salt-inducible kinase 3 protects tumor cells from cytotoxic T-cell attack by promoting TNF-induced NF-κB activation, J Immunother Cancer 10 (5) (2022).
[45] J.E. Bader, K. Voss, J.C. Rathmell, Targeting metabolism to improve the tumor microenvironment for cancer immunotherapy, Mol Cell 78 (6) (2020) 1019–1033.
[46] X. Mao, et al., Crosstalk between cancer-associated fibroblasts and immune cells in the tumor microenvironment: new findings and future perspectives, Mol. Cancer 20 (1) (2021) 131.
[47] L. Qin, J. Wu, Targeting anticancer immunity in oral cancer: drugs, products, and nanoparticles, Environ. Res. (2023) 116751.
[48] Y. Zhao, J. Du, X. Shen, Targeting myeloid-derived suppressor cells in tumor immunotherapy: current, future and beyond, Front. Immunol. 14 (2023) 1157537.
[49] S. Yan, Y. Zhang, B. Sun, The function and potential drug targets of tumour-associated Tregs for cancer immunotherapy, Sci. China Life Sci. 62 (2) (2019) 179–186.
[50] D.I. Gabrilovich, Myeloid-derived suppressor cells, Cancer Immunol. Res. 5 (1) (2017) 3–8.
[51] D. Peng, et al., Targeting TGF-β signal transduction for fibrosis and cancer therapy, Mol. Cancer 21 (1) (2022) 104.
[52] A. Chakravarthy, et al., TGF-β-associated extracellular matrix genes link cancer-associated fibroblasts to immune evasion and immunotherapy failure, Nat. Commun. 9 (1) (2018) 4692.
[53] D. Fukumura, et al., Enhancing cancer immunotherapy using antiangiogenics: opportunities and challenges, Nat. Rev. Clin. Oncol. 15 (5) (2018) 325–340.
[54] E. Picarda, K.C. Ohaegbulam, X. Zang, Molecular pathways: targeting B7-H3 (CD276) for human cancer immunotherapy, Clin. Cancer Res. 22 (14) (2016) 3425–3431.
[55] C.A. Chuckran, et al., Neuropilin-1: a checkpoint target with unique implications for cancer immunology and immunotherapy, J Immunother Cancer 8 (2) (2020).
[56] S. Chen, et al., The prognostic value and immunological role of CD44 in pan-cancer study, Sci. Rep. 13 (1) (2023) 7011.
[57] S. Wang, et al., STAT5A modulates gastric cancer progression via upregulation of CD44, Genomics 115 (3) (2023) 110638.
[58] D. Naor, et al., CD44 in cancer, Crit. Rev. Clin. Lab Sci. 39 (6) (2002) 527–579.
[59] X. Wang, et al., HDAC inhibitors overcome immunotherapy resistance in B-cell lymphoma, Protein Cell 11 (7) (2020) 472–482.
[60] C.Y. Wang, et al., Gene signatures and potential therapeutic targets of amino acid metabolism in estrogen receptor-positive breast cancer, Am. J. Cancer Res. 10 (1) (2020) 95–113.
[61] C. Yang, et al., A survey of optimal strategy for signature-based drug repositioning and an application to liver cancer, Elife (2022) 11.